BRITESPACE

High Brightness Semiconductor Laser Sources for Space Applications in Earth Observation

Project Coordinator	Ignacio Esquivias
Email	ignacio.esquivias@upm.es
Project website	www.britespace.eu
Grant Agreement	Number 313200 funded by the EC FP7-Space

FINAL PUBLISHABLE REPORT

Description of project context and objectives.

BRITESPACE project has been conceived for the design, realization and validation of a semiconductor laser transmitter to be used for the detection of carbon dioxide in future Earth Observation space missions. The proposed system consists of an Integrated Path Differential Absorption (IPDA) lidar based on a fully integrated semiconductor Master Oscillator Power Amplifier (MOPA). The project aims to demonstrate that high brightness semiconductor lasers can be used as optical sources in space applications which require simultaneously high power, beam quality and spectral purity.

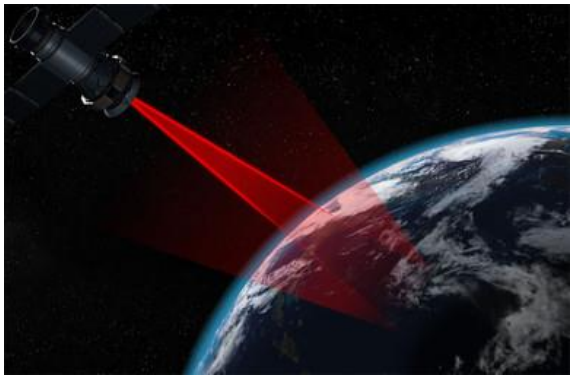

Artistic vision of BRITESPACE space-borne LIDAR mission.

An IPDA lidar basically works on the use of two different wavelengths for the measurement of CO_2 concentration: one wavelength is strongly absorbed (λ_{OFF}) and the other is lightly absorbed by the gas (λ_{ON}). In BRITESPACE the laser light is Randomly Modulated in Continuous Wave (RM-CW) in order to allow the determination of the height and differential absorption of the air column under measurement.

The main objectives of BRITESPACE Project can be summarized as follows:

- Definition of the requirements of the semiconductor laser source for future space-borne IPDA lidar mission.
- Definition, simulation and development of the complete RM-CW lidar system
- Design, fabrication and testing of the MOPA laser chip.
- Design, fabrication and testing of a space compatible Laser Module including the MOPA laser chips.
- Implementation of a Frequency Stabilization Unit and control electronics in the Laser Transmitter
- Laser Transmitter Performance Verification
- Integration of the Laser Transmitter into the complete PRM IPDA lidar system
- Test of the complete system on the ground in comparison with a pulsed IPDA lidar system

BRITESPACE Consortium:

Universidad Politécnica de Madrid (UPM), Spain	www.upm.es
III-V Lab, France	www.3-5lab.fr
Fraunhofer Institute for Laser Technology (ILT), Germany	www.ilt.fraunhofer.de
Alter Technologies (ATN), Spain	www.altertechnology.com
Deutsches Zentrum für Luft- und Raumfahrt (DLR), Germany	www.dlr.de
University of Bristol (UBRIS), United Kingdom	www.bris.ac.uk

CONTENTS

1. Introduction

Carbon dioxide (CO_2) is the major anthropogenic greenhouse gas contributing to global warming and climate change. The exchanges of CO_2 between the atmosphere and the natural or anthropogenic sources/sinks at the Earth's surface are still poorly quantified. A better understanding of these surface fluxes, and in particular their regional distribution, is required for appropriate policy making. At present, the concentrations of CO_2 are mainly measured in-situ at a number of surface stations that are unevenly distributed over the planet. Air-borne and space-borne missions have the potential to provide a denser and better distributed set of observations to complement this network. Space-borne lidar systems require laser transmitters with very good performance in terms of output power, beam quality, conversion efficiency, long term reliability and environmental compatibility. Additionally, spectral purity and stability are required for gas sensing. The availability of suitable laser sources is one of the main challenges in future space missions for accurate measurement of atmospheric CO_2.

Typical laser sources currently used in lidars systems are solid state lasers working in pulsed regime, emitting ns pulses with high energy at low to medium repetition rate (typical values are 10-50 ns, ~10-50 mJ, 50-200 Hz) [1,2]. Although these laser systems have demonstrated the high average power, high laser beam quality and frequency stability required by the application, it is at the expense of a bulky system with low wall plug efficiency, which is a main concern for space-borne applications. Numata et al. [3] have investigated on hybrid Master Oscillator Power Amplifiers (MOPAs) combining a Distributed Feedback (DFB) semiconductor laser as seed laser and Erbium Doped Fiber Amplifiers (EDFA) working in pulsed conditions in the context of NASA mission ASCENDS. However, the use of active optical fibers in space applications requires specific attention to the radiation shielding, orbit and the duration of the flight, since it is known that EDFAs have low radiation hardness.

Recently, a new generation of high brightness semiconductor lasers based on tapered geometry has demonstrated relatively high average power levels together with a good beam quality [4-6]. These devices are emerging candidates for its direct use in space lidar systems. Semiconductor lasers have clear advantages over other laser types in terms of compactness and conversion efficiency (up to 75%). They present high reliability and good radiation hardness for most space applications. They can be fabricated with emission wavelengths ranging from Ultra-Violet up to Far-Infrared, and those with appropriate design can be tuned over several tenths of nanometers. Broad area semiconductor lasers can achieve more than 20 W CW, but they suffer from a poor beam quality. Tapered semiconductor lasers [4,5] also known as flared unstable cavity lasers, have demonstrated both high power and good beam quality at different wavelengths. These devices consist of a ridge waveguide (RW) section and a tapered section. The single spatial mode of the RW section is launched into the tapered section where it is amplified while keeping its single mode profile. Improved epitaxial structures, together with the use of long cavity designs have led to single-emitter tapered lasers providing more than 10 W with a low beam propagation ratio M^2 at 1060 nm and 980 nm [4,5]. The spectral properties of tapered lasers are similar to those of BA lasers, with multiple modes and broad and unstable emission spectra, but they can be enhanced by the use of a Distributed Bragg Reflector (DBR) to select a single longitudinal mode [5]. The integrated MOPA architecture, consisting of either a DFB or a DBR laser as oscillator and a tapered semiconductor amplifier, presents advantages for those lidar applications requiring good spectral properties. Integrated DBR MOPAs have demonstrated up to 12 W in CW operation at 1064 nm [6].

Standard Integrated Path Differential Absorption (IPDA) lidar systems use high peak power optical pulses at two sounding frequencies to calculate the column averaged gas concentration [7]. The limited peak power of semiconductor lasers in comparison with solid state or fibre lasers requires a different approach more suited to the particular emission properties of these lasers. In the framework of the European FP7-Space project BRITESPACE we propose an all-semiconductor laser source based IPDA lidar system for column-averaged measurements of atmospheric CO_2 in future satellite missions. The Random Modulated Continuous Wave (RM-CW) approach has been selected as the best

suited to semiconductor lasers [8,9]. The transmitter design is based on two monolithic MOPAs, providing the on-line and off-line wavelengths close to the selected CO_2 absorption line around 1.57 μm. Each MOPA consists of three sections: a frequency stabilized Distributed Feedback (DFB) master oscillator, a bent modulator section and a tapered amplifier [10]. The use of this original structure aims to fulfill the requirements of performance by the IPDA system in terms of relatively high power, frequency stability and good beam quality. The DFB section is accurately frequency stabilized by an external opto-electrical feedback loop through the Frequency Stabilization Unit (FSU). The modulator section is introduced for the implementation of the RM-CW technique in the proposed IPDA system. Finally, the geometry of the tapered SOA is optimized in order to provide a high brightness output beam with sufficient power and beam quality.

More than 400 mW ouput power with a SMSR higher than 45 dB and stable emission have been demonstrated at room temperature. In addition, modulation at tenths of MHz using the modulator section has been achieved, showing its suitability for the RM-CW lidar application. On the side of the receiver, our modeling and simulations indicate that the major noise contribution comes from the ambient light. For this reason narrow band optical filters are used in the detection together with high sensitivity and low noise single photon counting techniques. Due to technical problems, the fabricated MOPAs were not integrated in the complete RM-CW IPDA lidar system. In order to perform the proof-of-concept of the approach the lidar system was completed with commercial DFB lasers and an EDFA. As far as we know, the obtained results demonstrate for the first time the validity of an IPDA lidar system based on the RM-CW of semiconductor lasers, together with Single Photon Counting at the receiver.

In this report, we summarize the activity carried out by the BRITESPACE consortium in the last three years about the design, modeling, fabrication and characterization of the complete RM-CW IPDA lidar system. The report is organized as follows. In Section II, the theoretical analysis of the RM-CW IPDA lidar system is presented. As a consequence of this analysis, the system requirements are identified and discussed. Section III is devoted to the design, fabrication and characterization of the laser transmitter. Special emphasis is given to the integrated MOPA proposed, the FSU and the laser module. Section IV is devoted to the design and fabrication of the receiver based on single photon counting. In addition, first CO_2 detection tests are discussed. In Section V, the results of the different test campaigns are shown. The campaigns were devoted to the validation of the FSU and to perform CO_2 measurements of the BRITESPACE RM-CW IPDA lidar system in comparison with CHARM-F [11] pulsed system. Finally, conclusions are given in Section VI.

For completeness, the list of the articles published and contributions to conferences are given in Appendix A and B, respectively. A brief summary of the workshops organized by the BRITESPACE consortium is also included in Appendix C. A glossary of terms is written in Appendix D. Finally, the list of the technical personnel involved in the BRITESPACE project is given in Appendix E.

2. System modeling and requirements

2.1. Theoretical model

An IPDA lidar can provide column-averaged CO_2 measurement by sounding the atmosphere at two wavelengths which are relevant for the gas under study: one wavelength is set near the center of a CO_2 absorption line (on-line channel, λ_{on}) and the other is set close to but off the same line (off-line channel, λ_{off}) as can be seen in the inset of Fig.1 (a). Both wavelengths are close enough to exhibit almost identical aerosol attenuations, but will exhibit different CO_2 absorptions. The attenuation from CO_2 molecules can be calculated by the power ratio of the back-scattered signals at the end of the optical path and can be converted into a column-averaged mixing ratio thanks to the knowledge of the path length from the round-trip time delay. The Differential Absorption Optical Depth (DAOD) quantifies the molecular absorption by the CO_2 along the path between the scattering surface and the instrument. It can be written as

$$\mathrm{DAOD} = \frac{1}{2}\ln\left(\frac{E_{on}\,R_{off}}{E_{off}\,R_{on}}\right) = \int_0^Z \left(\sigma_{on}(z) - \sigma_{off}(z)\right) n_{CO2}(z)dz\,, \tag{1}$$

where $E_{on,off}$ are the emitted on- and off-line energies, $R_{on,off}$ are the received on- and off-line echoes, n_{CO2} is the CO_2 density and $\sigma_{on,off}$ denotes the altitude dependent effective cross-section. In the particular case of using RM-CW, the transmitted signal is a Pseudo Random Bit Sequence (PRBS) as shown in Fig. 1 (b). The off-line signal is delayed respect to the on-line signal in order to avoid cross-talk [12].

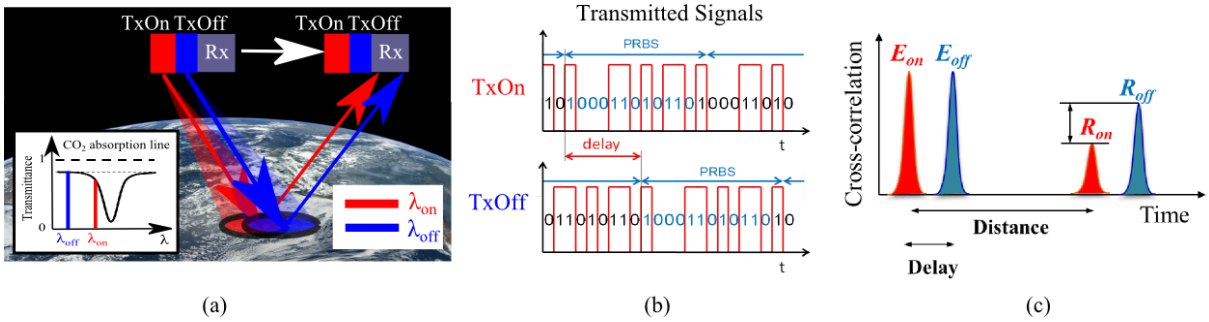

Fig. 1: Illustration of the RM-CW lidar technique. (a) Principle of operation of an IPDA lidar. Inset: Position of the on-line and off-line selected frequencies with respect to the CO_2 absorption line. In our case the absorption line is around 1.57 μm in order to minimize the interference from the H_2O lines. (b) Transmitted PRBS signals. Notice the delay on the PRBS code between the off-line and on-line signals. (c) Cross-correlation between the emitted PRBS and the received signals allowing distance and differential absorption measurements.

An N-bit PRBS can be represented as $a[i] \in \{0,1\}$. Assuming single photon detection, the measurement of the cross-correlation $C[i]$ between the PRBS (the optical detected signal) with its bipolar sequence described by $a'[i] = a[i] - \bar{a}[i] \in \{-1,1\}$ (the electrical reference signal) for both on-line and off-line wavelengths provides the DAOD. When a PRBS $a[i]$ of the length $N = 2i_m$ is used for the on-line signal $a_{on} = a[i]$, the off-line code can be obtained by cyclically shifting the PRBS as $a_{off} = a[i - i_m]$. This approach allows the returns of both wavelengths to be separated and distinguishable in the cross-correlation result. At the detector, apart from the signal counts, ambient light and detector dark counts are also collected. The combined cross-correlation result can be written as

$$C[i] = \left(n_{on}[i] + n_{off}[i] + n_{amb}[i] + n_{\mathrm{det}}[i]\right) \otimes a'[i]\,, \tag{2}$$

where

$$n_{on,off}[i] = 2\,P_{on,off}\,G_{on,off}\,t_c\,\eta_e\,a_{on,off}[i - \tau / t_c]\,, \tag{3}$$

$$n_{amb} = \eta_e\,t_c\,L_s\,\Delta_\lambda\,A_s\,\frac{A_r}{Z^2}\,\mathrm{e}^{-OD_0}\,, \tag{4}$$

$$n_{\mathrm{det}} = k_{dc}\,t_c\,. \tag{5}$$

$P_{on,off}$ is the initial average power of the on- and off-line transmitted signals, t_c is the bit time or chip-time, η_e denotes the conversion coefficient from incident photon numbers to detections of photo-electrons (including the optical and detector efficiencies) and

$$G_{on,off} = \alpha\,\frac{A_r}{Z^2}\,\mathrm{e}^{-2OD_{on,off}}\,, \tag{6}$$

with the total column optical path written as

$$OD_{on,off} = OD_0 + \int_0^Z \sigma_{on,off}(z)\, n_{co2}(z) dz\,, \tag{7}$$

where α is the albedo for the ground (approximated by a Lambertian surface), A_r is the receiving telescope area, Z is the ground distance $Z = c\tau/2$, being τ the flight time, $OD_{on,off}$ denote the total column optical depth, including a losses wavelength-independent term OD_0. The total and differential absorptions are related through $\mathrm{DAOD} = OD_{on} - OD_{off}$.

With respect to Eq. (4) and (5), L_s denotes the Nadir solar spectral radiance; Δ_λ represents the bandwidth of the optical filter at the detector; A_s is the ground surface area covered by the detector field-of-view, that relates to the receiver field-of-view θ_{fov} of the receiver by $A_s = 1/4\pi\theta_{fov}^2 Z^2$; A_r / Z^2 denotes the solid angle of the receiver telescope.

As shown in Fig. 1 (c), the sample of the emitted energies are recoded at the initial bins as the photon numbers $E_{on,off}$, while the last returned bins record the total received photon number for the on and off-line wavelengths $R_{on,off}$; They can be written as

$$R_{on,off} = C_{on,off}[\tau/t_c] = 2\,N\,P_{on,off}\,G_{on,off}\,t_c\,\eta_e\,. \tag{8}$$

On the other hand, the total dark counts and ambient counts integrated in a cross-correlation bin can be further denoted as $R_{amb} = N\,n_{amb}$ and $R_{\mathrm{det}} = N\,n_{\mathrm{det}}$ respectively.

The quantity of scientific interest, the dry-air volume mixing ratio of CO_2, vmr_{CO2}, is related to n_{CO2} and the density of dry air n_{air} via $vmr_{CO2}(z) = n_{CO2}(z)/n_{air}(z)$. In fact the obtained DAOD is proportional to a weighted average of vmr_{CO2} over the whole column which is referred as XCO_2,

$$XCO_2 = \int_0^Z vmr_{CO_2}(z)\frac{WF(z)}{\int_0^Z WF(z)dz}dz = \frac{DAOD}{IWF}\,, \tag{9}$$

where the weighting function WF is described by

$$WF(z) = n_{air}(z)\left(\sigma_{on}(z) - \sigma_{off}(z)\right), \tag{10}$$

where the density of air n_{air} can be obtained from the ideal gas law, and the altitude dependent cross-section $\sigma_{on,off}$ can be calculated from data obtained from the HITRAN database [13]. The details on the model developed based in a full-waveform simulation, where effects such as linewidth broadening, Doppler shift and topographic variations are included, will be published elsewhere [14]. To summarize, XCO_2 can be calculated from the following information: (a) the instrument measurement by the energy ratio of the received on- and off-line wavelengths; (b) the orbit altitude to ground distance Z, also derived from the lidar returns themselves; and (c) Numerical weather prediction and spectroscopic auxiliary data. By proper selection of the sounding on and off-line wavelengths possible measurement biases due to atmospheric water vapor can be significantly reduced [15].

The variance of the on-line at the peak of cross-correlation V_{on} and so forth for the off-line variance V_{off} is obtained as

$$V_{on,off} = R_{on,off} + R_{off,on} + R_{amb} + R_{det}\,, \tag{11}$$

Consequently on- and off-line SNRs can be estimated,

$$SNR_{on,off} = \frac{R_{on,off}}{\sqrt{R_{on,off} + R_{off,on} + R_{amb} + R_{\det}}}. \quad (12)$$

With the SNRs formulated, assuming Gaussian approximation to Poisson noise, the CO_2 retrieval precision can be estimated by Gaussian error propagation. The CO_2 detection precision can be simplified to

$$\Delta xco_2 = \sqrt{\left(\frac{\delta xco_2}{\delta R_{on}}\right)^2 V_{on} + \left(\frac{\delta xco_2}{\delta R_{off}}\right)^2 V_{off}} = \frac{\sqrt{SNR_{on}^{-2} + SNR_{off}^{-2}}}{2\,IWF}. \quad (13)$$

The theoretical model defines the CO_2 retrieval precision (random error) in relation to varying system parameters. An extensive study of the model led to a good understanding of the underlying principles, yielding to a baseline system configuration. To optimize a large set of related parameters, an initial condition was defined. This is set according to the intuitive understanding of the IPDA lidar approach with reference to pulsed systems from [7]. The set of requirements resulting from the analysis of the model are indicated in Tab. 1 and 2 of the next section.
In summary, the results indicate that for the proposed system architecture, major noise contributor is the ambient light shot noise and the detector dark count in the RM-CW scheme. From this, to use a narrow band-pass filter at the receiver and a single photon detector is needed. Fig. 2 shows the CO_2 retrieval precision for three types of surface with respect to (a) on-line center wavelength and (b) filter bandwidth. For more details we refer the reader to [14].

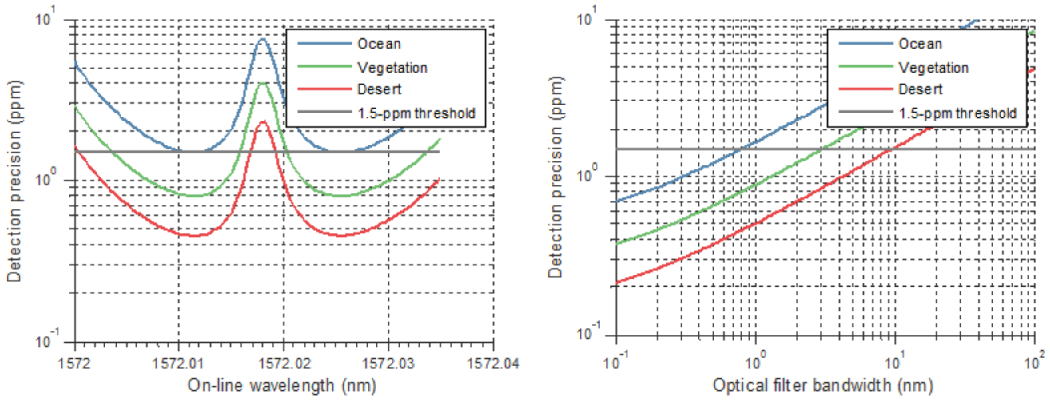

Fig. 2: CO_2 retrieval precision for three types of surfaces with respect to (a) the on-line center wavelength and (b) the receiver optical filter bandwidth.

2.2. Application requirements

The architecture of the BRITESPACE Laser Transmitter has been defined according to the performance requirements imposed by the implementation of the final IPDA lidar. The most challenging requirements are high power output, good beam quality and high frequency stabilization. The core solution addressing these issues is the use of two fully integrated semiconductor MOPAs, with a novel three-section structure, consisting of a DFB laser, a modulator and a tapered amplifier section. Each MOPA works at one of the two emission wavelengths required for CO_2 detection. Long term frequency stability, low frequency noise and tunability are assured by a FSU with offset frequency, locking scheme and opto-electronic feedback referred to a CO_2 reference cell. The output beam profile is optimized by the geometrical design of the MOPAs, and the two output beams are collimated, combined and sent to output with the use of a specific beam forming optics layout and telescopes. The scheme of the laser transmitter is shown in Fig. 3.

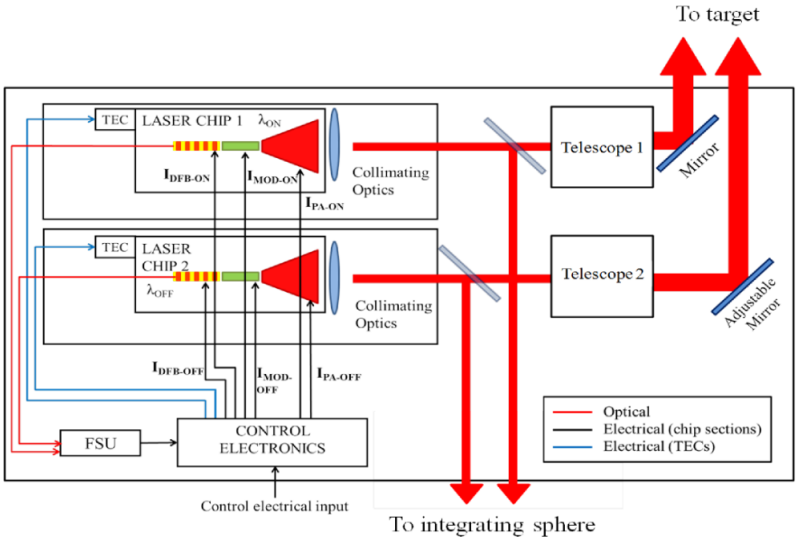

Fig. 3: Schematics of the laser transmitter. TEC: Thermoelectric cooler. FSU: Frequency Stabilization Unit.

The schematic of the full RM-CW IPDA lidar system is shown in Fig. 4. It includes an integrating sphere to mix and to homogenize a fraction of the emitted power and the received power and a short-wave infrared camera (SWIR) to facilitate the pointing connected to the telescope and the photon counting detector.

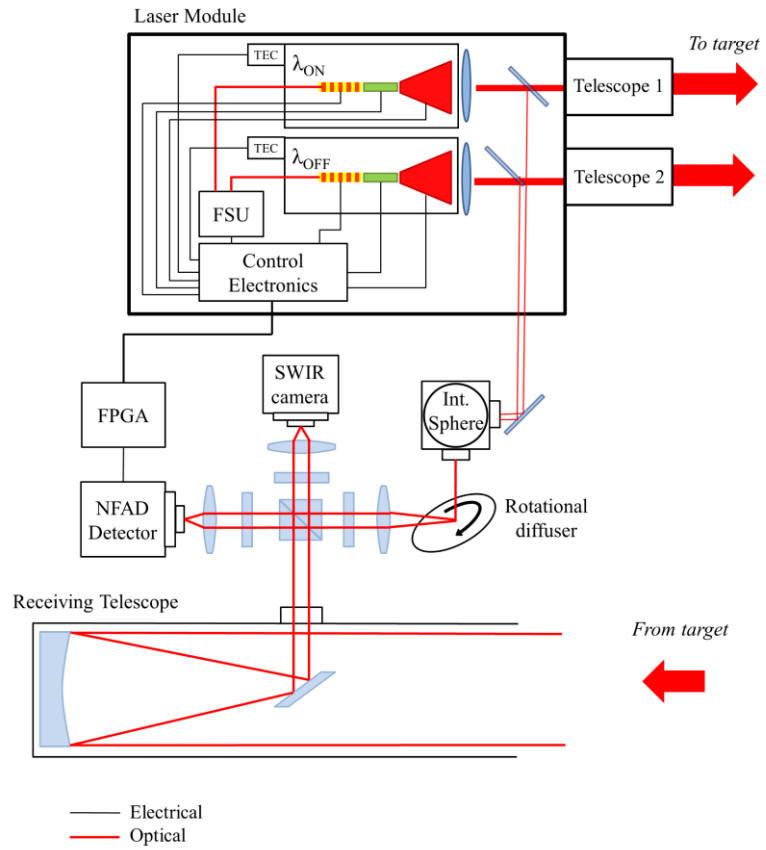

Fig. 4: Schematics of the proposed RM-CW IPDA LIDAR instrument. NFAD: Negative Feedback Avalanche Diode.

The analysis of the laser transmitter specifications to achieve the general goal is based on the analytical model described in Section 2.1. The model is used to estimate the precision of the complete system for different values of the system parameters. As expected, the XCO_2 retrieval precision depends on all the involved parameters. In consequence, it appears to be convenient to express the laser transmitter specifications for a baseline set of system parameters which are collected in Tab. 1.

Platform and environment	
Orbit altitude	450 km.
Ground velocity	7 km/s
Ground mixing ratio	410 ppm
Receiver and detector	
Telescope area	1.8 m^2
Filter bandwidth	800 pm
Detector type	Single photon detector
Dark count	100 kcps
Conversion coefficient	40%

Tab. 1: Parameters of the platform and receiver used as baseline for the definitions of Laser Transmitter specifications shown in Tab. 2.

According to the model calculations, the required retrieval precision of 1.5% in worst conditions (ocean) can be achieved with baseline parameters and the specifications for the laser transmitter collected in Tab. 2.

During third year, the results obtained in the spectral broadening of the MOPA devices under modulation indicated that the spectral specifications are not appropriate. The emitted spectra cannot be characterized by a spectral linewidth but by a complete measurement. If the spectral broadening is deterministic, repetitive and can be accurately characterized, it can be introduced in the retrieval algorithm to get the XCO_2 mixing ratio. The accuracy in the determination of the spectral properties of the modulated MOPA should be further investigated. In consequence the specifications have been modified, including non-applicable in the "spectral bandwidth" and tbd (to be determined) in the "accuracy of spectral characterization".

3. Laser transmitter

3.1. Master Oscillator Power Amplifier (MOPA)

Design

A set of two InGaAsP/InP monolithic MOPAs is proposed as the main building block of the Laser Transmitter. Each MOPA is a three section device, consisting of a frequency stabilized DFB laser acting as a master oscillator, a modulator section, and a tapered amplifier. The use of this original structure aims to fulfill the performances required by the IPDA system in terms of high power, frequency stability and good beam quality. In this sense, the DFB section is accurately frequency stabilized in an external opto-electrical feedback loop through the FSU. The modulator section is introduced for implementation of the RM-CW technique in the proposed IPDA system. Finally, the geometry of the tapered amplifier is optimized in order to provide high brightness output beam with sufficient power and beam quality.

More in detail, three different geometries were proposed for the Laser Chip implementation. They were based on: straight, tilted and bent designs, shown in Fig. 5. The straight geometry consists of a standard structure in which the oscillator, modulator and amplifier sections are in-line with the propagation axis and perpendicular to the output facet (i.e. the tilt angle is 0º). The tilted and bended geometries are proposed in order to minimize undesired optical feedback from the amplifier section to

the DFB oscillator. In fact, standard straight monolithically integrated MOPAs are typically characterized by non-linear behavior due to compound cavity effects from residual reflectivity at the amplifier output facet [16, 17].

A. SPECTRAL			
Nominal sounding frequencies	○ on-line channel ν_{on} 190.704710 THz. ○ off-line channel ν_{off} 190.694980 THz.		
On-line channel tunability			+/- 350 MHz.
On-line and off-line frequency stability (over 10s)		*maximum*	*desirable*
○ on-line channel		0.1 MHz	0.02 MHz
○ off-line channel		100 MHz	20 MHz
Spectral linewidth			Non-applicable *
Linewidth knowledge			+/- 5 MHz
Accuracy of spectral characterization			tbd **
Effective Spectral Purity			≥ 99.9%
On-line and off-line frequency stability (over 10s)		*maximum*	*desirable*
○ on-line channel		0.1 MHz	0.02 MHz
○ off-line channel		100 MHz	20 MHz
B. POWER			
Average Optical Output Powers			
○ *on-line channel* $<P_{OPT-ON}>$			≥ 2 W
○ *off-line channel* $<P_{OPT-OFF}>$,			≥ 1 W and ≤ 1.5 W
Wall-plug Efficiency WPE_{ON}, WPE_{OFF}			≥ 20%
Power stability (rms)	*short term (over 10 sec.) PSST*		≤ 2 %
	long term (over 24 hours) PSLT		≤ 10 %
C. BEAM			
Polarization Extinction Ratio (PER)			≥ 13 dB
Beam Propagation Factor M^2 (slow axis)			$M^2 \leq 3$
Full Beam Divergence (both axes)			≤ 75 µrad
Beam Pointing Stability (rms)			≤ 120 µrad
D. MODULATION			
Pseudo Random Modulation Repetition Frequency (f_{MOD})			≤ 5 kHz
Chip time			= 40 ns
Modulation format			1:1 NRZ

Tab. 2: Final laser transmitter specifications. *, ** The accuracy in the determination of the spectral properties of the modulated MOPA should be further investigated. See text for details

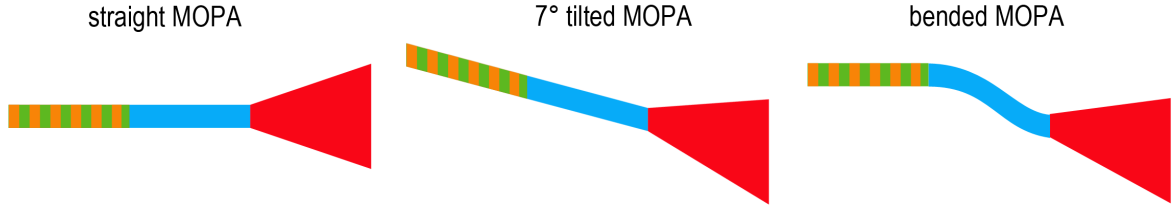

Fig. 5: Straight, tilted and bent geometry designs for Laser Chip fabrication.

The design of the epitaxial structure of the devices is optimized in order to decrease the internal losses, which are relevant on InP based devices, and reduce the output beam divergence in the vertical direction. It is based on a dilute slab asymmetrical cladding approach [18] and multiple Quantum Well (QW) active region. Results on fabricated broad area lasers with the mentioned epitaxial design have shown promising results in terms of low internal losses (7.3 cm^{-1}), low threshold current density (<480 Acm^{-2}), low vertical divergence (32º) and high internal quantum efficiency (93%). Finally, after the first run of fabricated devices, the bent MOPA was chosen as the best suited in order to avoid modal instabilities as it will be shown in next sections and in agreement with [19].

Simulation

The simulation of the devices has been carried out via two approaches: a) A Quasi-3D Beam Propagation Method (BPM) that includes full electro-thermal and optical description of the device that has been used to simulate the modulator and amplifier sections. And b) Spatio-temporal Travelling Wave Models (TWMs) that allow the dynamical simulation of multi-section devices that has been used to investigate instabilities of straight MOPAs [20] and the effect of modulation in the three-section bent MOPA [21].

A Quasi-3D simulation tool for tapered lasers was adapted to tapered Semiconductor Optical Amplifiers (SOAs) in order to optimize the geometry of the devices [22]. As a first step, the tool was calibrated to reproduce the characteristics of a typical first run MOPA device, see Fig. 6 (a). This simulation was used a posteriori as reference in order to propose improvements in the fabrication. As examples, Fig. 6 (b) shows the confinement factor effect in the thermal behavior of the device. Fig. 6 (c) shows the effect of using different mounting (p-down and p-up) for the device and its impact in the thermal behavior of the device and consequently in the reached output power.

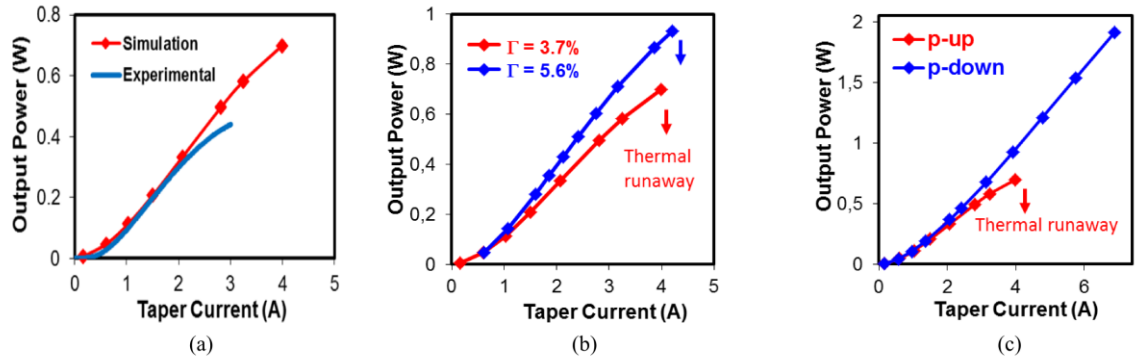

Fig.6: Simulations from a Quasi-3D simulation tool for SOAs. (a) Experimental (blue) and simulated (red) Power-Taper current characteristics of a typical run #1 MOPA. This simulation is used as a reference in the following. (b) Effect of the confinement factor. (c) Effect of using different mounting (p-down and p-up) for the device.

Experimental results

III-V Lab has fabricated 3-section monolithic MOPAs on InP, see Fig. 7 (a) and (b). The 1st section is the oscillator (DFB laser), the 2nd section is a modulation section (MOD) and the 3rd section is a flared power amplifier (PA). Best results were obtained with a bent modulator section in order to reduce the facet reflections at the end of the amplifier. We observed that this architecture is more stable than the straight one, where all the sections are aligned. We observe stable emission around 1583 nm with a side mode suppression ratio better than 45 dB. Fig. 7 (c) shows the optical power as a function of the amplifier current I_{PA} (I_{DFB} = 0.4, I_{MOD} = 300 mA). The maximum optical power is 420 mW at 18ºC (I_{PA} = 3 A); by decreasing the temperature to 12 and 6°C, we have obtained a maximum output power of 510 and 600 mW respectively. Fig. 7 (d) shows the optical spectra dependence on I_{DFB} for I_{MOD} = 300 mA and I_{PA} = 3 A. The laser exhibits multimode operation close to the threshold (DFB laser without phase-shift) and single-mode operation without any mode hopping from 300 to 500 mA. [10]

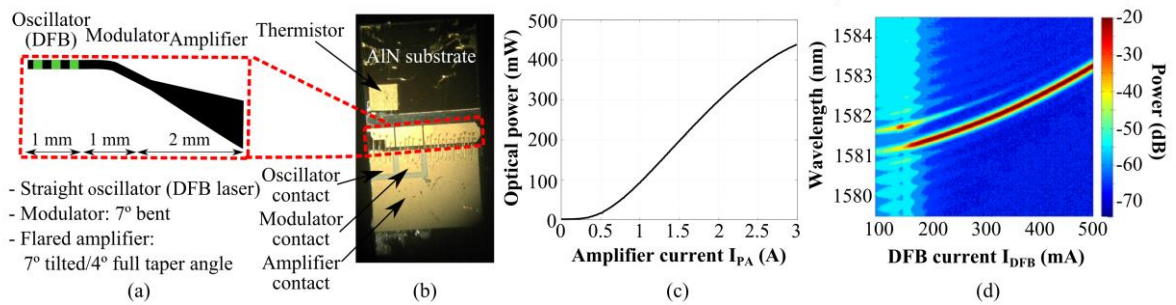

Fig. 7: Fabricated 3-section bent MOPAs. (a) Schematics of the device. (b) Photograph of the device. (c) Power vs PA current characteristics at T = 18 ºC. (d) Optical spectrum while varying the DFB current.

In order to modulate the laser output while maintaining its operation frequency, the current of the MOD section is modulated. Fig. 8 (a) shows the optical power as a function of the MOD section current, I_{MOD} (I_{DFB} = 300 mA, I_{PA} = 2.5 A). It can be seen that for suppressing the output power, we need to extract current from the system. This measurement was performed using a four quadrant current source. Fig. 8 (b) shows a time trace while modulating the MOD section with a square signal at the frequency required by the application, f = 12.5 MHz. Fig. 8 (c) shows the eye diagram obtained from the laser module while exciting the MOD section with a square signal at 12.5 MHz.

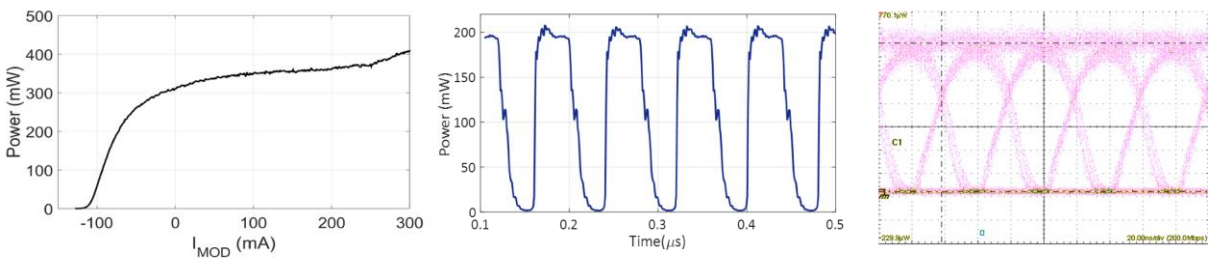

Fig. 8: Modulation of the 3-section MOPA. (a) Power versus modulator current characteristics in CW. (b) Output power obtained by exciting the modulator with a square signal at the frequency required by the application (12.5 MHz). (c) Eye-diagram obtained from the laser module optical output at 12.5 MHz.

Preliminary results on the modulation characteristics of the MOPA devices have shown that the spectra found seem to correspond to frequency modulation. The typical shape obtained from a composition of Bessel functions of first kind was clearly seen. The spectral properties of the modulated MOPA should be further investigated

Radiation test

Radiation test were performed in order to assure space conditions reliability. One MOPA mounted according to the radhard specifications and two unmounted chips were submitted to the proton radiation test (for both: displacement damage and TID) as can be seen in the Tab. 3.

Equivalent TID (krad)	Fluence (p/cm2)	Flux (p/s·cm2)	Time (s)	MOPA Sample
26	8.88E+10	1.48E+09	60.03	1
50	1.71E+11	1.48E+09	115.44	2
100	3.42E+11	1.48E+09	230.89	3

Tab. 3: Radiation test plan samples

Post-radiation characterization revealed that the two MOPAs which were not survived the radiation test up to the equivalent doses shown in table above and showed degradation neither in power-current

nor voltage-current characteristics, as can be seen in Fig. 9. The threshold current remained also unchanged. This is a promising result proving that material and layer structure chosen for the MOPAs are correct and can withstand radiation equivalent TID up to 50 krad. The mounted MOPA has degraded after the radiation test up to 100 krad, but it is not proven if the radiation was the main reason of degradation or the device has failed like other MOPAs.

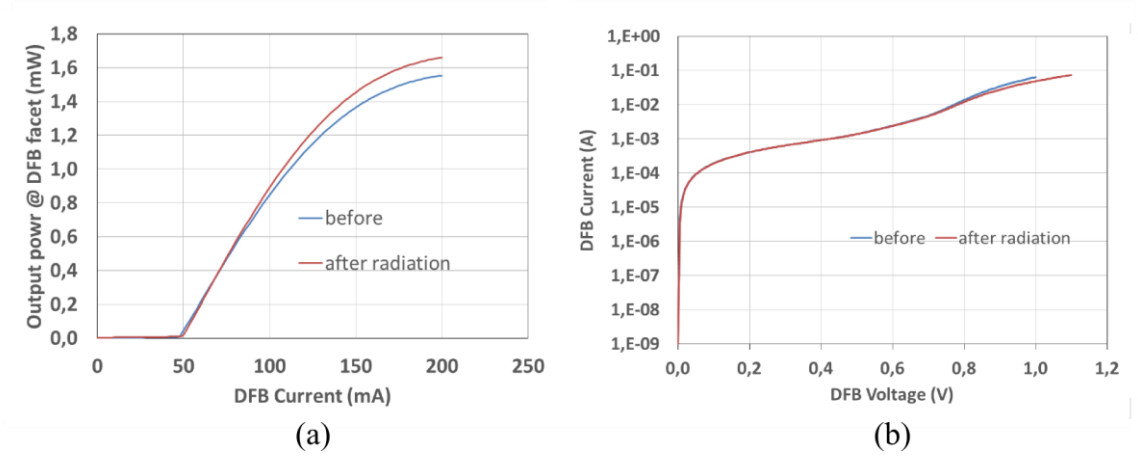

Fig. 9: (a) Power-current and (b) voltage-current characteristics of MOPA before and after the radiation test.

3.2. Frequency Stabilization Unit (FSU)

IPDA lidar systems require high frequency stabilization for accurate estimation of gas molecule concentration, in order to have precise measurement of the detected power ratio at the selected absorption line [7]. We propose the use of two opto-electrical feedback loops for the stabilization of the on- and off- channels emitted by the MOPAs. A simple scheme, showing the selected design for the Frequency Stabilization Unit (FSU), is shown in Fig. 10.

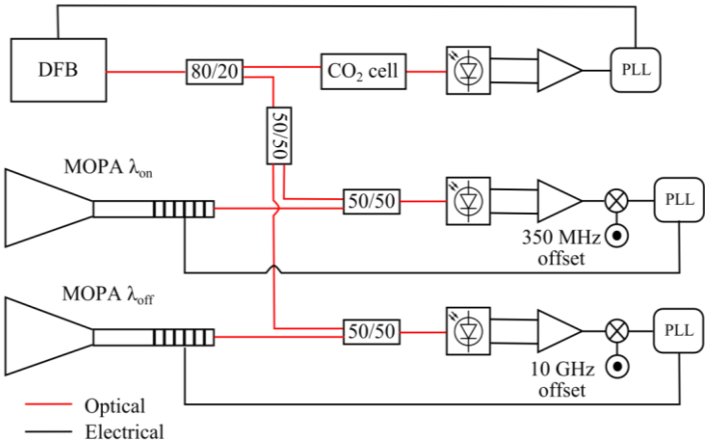

Fig. 10: Schematics of the Frequency Stablization Unit (FSU).

Light emitted from the back facet of the DFB section of the on- channel MOPA will be collected through a lensed SMF fiber and sent to a 50:50 fiber coupler. One of the output port of the coupler is sent to the on-channel locking feedback loop and the other is combined with the light emitted from the back facet of the off- channel MOPA with a second 50:50 fiber coupler. The on-channel MOPA will be locked to the selected CO_2 absorption line using a multi pass CO_2 reference cell and a custom feedback loop based on commercial available laser frequency locking equipment. A second feedback loop will be used to stabilize the beat note of the on- and off- channel signal at a fixed 10 GHz offset. The on- and off- channels frequency locking loops are schematically depicted in Fig. 10, where only

the main components are shown: the CO_2 reference cell, the 10 GHz signal generator and the Phase Locked Loop (PLL).

3.3. Laser module

The laser transmitter has been defined in Section 2.2, in particular Fig. 3 shows the schematics of it. In this section the fabrication of the laser module is discussed. The radiation emitted by the tapered amplifier facet is astigmatic, i.e. it has different virtual sources (and different angles of divergence) for the fast axis (vertical direction) and for the slow axis (horizontal direction) [10]. Due to this characteristic an optical system for the collimation of the tapered amplifier output must consist of two lenses: An aspheric lens and a cylindrical lens. The first lens is for collimation of the fast axis and intermediate focusing of the slow axis while the second cylindrical lens collimates the slow axis without affecting the fast axis beam. On account of the bent geometry of the laser chips (see Section 3.1), the emitter is tilted in the slow axis in order to achieve perpendicular propagation. The back facet output of the MOPA laser chips are sent to the FSU through standard Single Mode Fibers (SMF) for frequency stabilization. The radiation emitted from the back facet of the DFB is expected to be diffraction limited, and therefore can be coupled into a lensed SMF aligned to the DFB back facet. Partially reflective mirrors are used in order to allow power monitoring for each MOPA with two photodiodes and to send the reference signal to the integrating sphere. The laser beams from the two laser chips are placed close to each other using the adjustable mirrors placed after the telescopes, for minimizing footprint errors in IPDA detection. The CAD design shown in Fig. 11 (a) and the subsequent fabricated module, which photograph is shown in Fig. 11 (b), is intended to be used to perform the proof-of-concept and various on earth tests, for this reason accessibility to the different parts of the transmitter as well as versatility has been improved with respect to other designs more oriented to space compatibility.

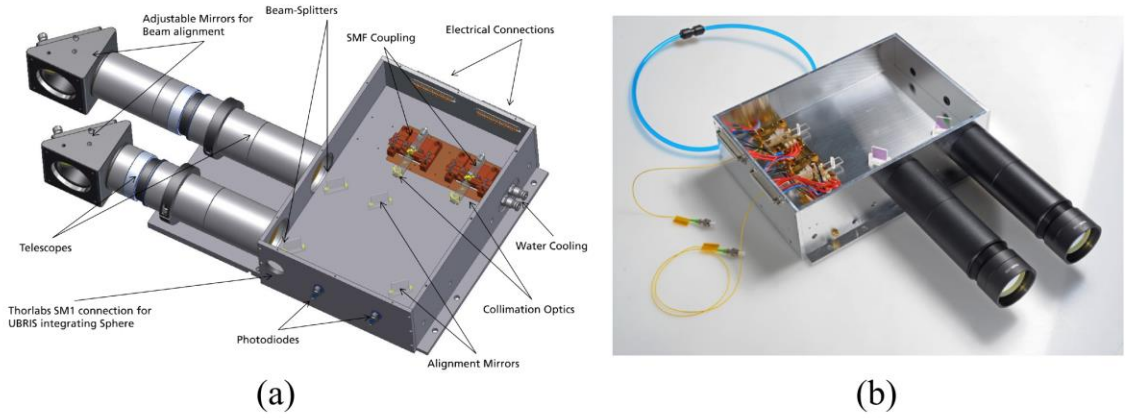

Fig. 11: BRITESPACE laser module. (a) CAD design. (b) Photograph.

Fig. 12 shows the power current characteristic obtained from the laser module. The optical-optical overall efficiency of the module is around 90.2 %. In terms of beam divergence, for the fast axis: it was obtained 1.3 mrad in collimated beam, with 11x magnification in telescope ~120 μrad. While for the slow axis: it was obtained 2.3 mrad in collimated beam, with 11x magnification in telescope ~ 210 μrad.

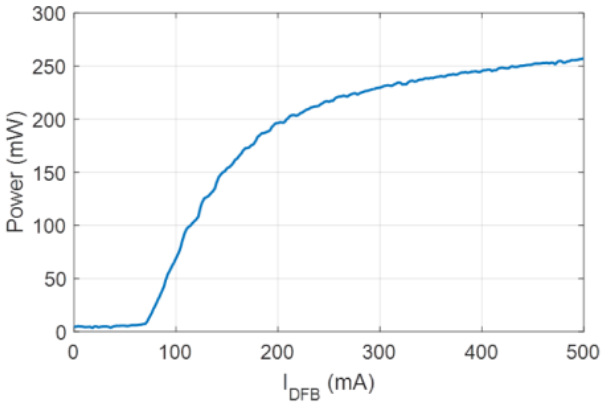

Fig. 12: Power current characteristic from the laser module.

4. Single photon counting detection

4.1. Single photon receiver

For space-borne applications, the received light power is estimated to be less than picowatt. A single photon detector is used to improve the SNR over the classical linear mode detectors. For free-running detection of single photons in 1.5 µm region, we have identified the Negative Feddback Avalanche Diode (NFAD) to be the most suitable detector for the application. We have developed in-house our own single photon detector unit as commercial detectors do not satisfy our need for high saturation count rate. A scheme of our single photon detector is plotted in Fig. 13 (a). A bias voltage of 70 V is applied to the diode. The chip temperature is stabilized to -20 ºC with TEC. Two stages of amplifiers of a combined 40 dB gain rise the avalanche signal level to 100 mV and adequate for threshold then converted to digital trigger into the FPGA. Our detector achieves 5 Mcps with 100 kcps dark count.

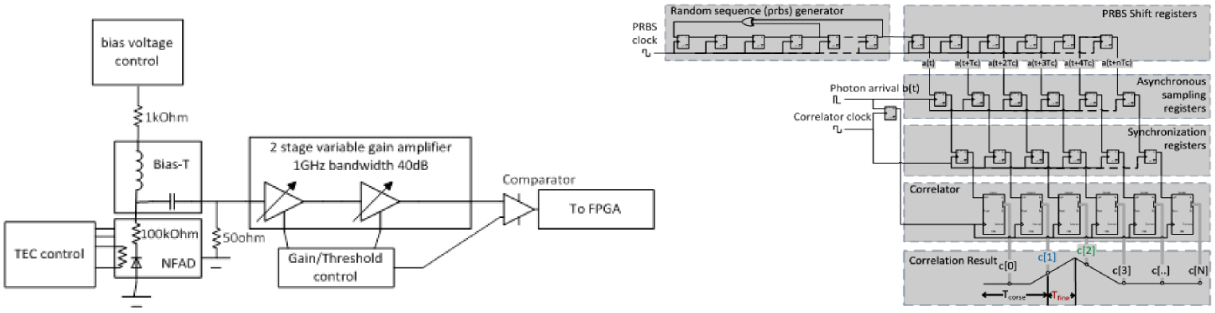

(a) (b)

Fig. 13: (a) In-house developed signal photon NFAD detector. (b) PRBS code generation and correlator implemented in the FPGA

Alternatively to other correlators, our FPGA implementation of the single photon correlator is based in an asynchronous design, see Fig. 13 (b). First of all the PRBS is generated by some shift registers, a shift register delay line then records this signal, once a photon is received, the rising edge of the photon trigger will latch the shift register contents into the flip-flop, subsequent to this layer a synchronization registers layer is needed to deal with meta-stability. The last layer is the correlator elements that are just counters which counts up with `1' and counts down with `0'. The results shown a triangle where the addition of c[1] and c[2] indicate the number of correlated photons. It should be noticed too, that in the detector non-linearity is cancelled due to ratio between the off-line and the on-line received signals.

4.2. CO_2 detection test

To evaluate the effectiveness of the detection system we implemented the experiment shown in Fig. 14. An integrating sphere is used as gas cell, and we show the absorption with respect to laser frequency changes when CO_2 is injected into the integration sphere. Fig. 14 (a) shows the scheme of the experiment used for CO_2 detection test. A wavelength tunable DFB laser (Thorlabs LS5000 series module) for DWDM applications is modulated with an acoustic optical modulator (AOM). The PRBS modulation is generated by the FPGA, the modulated light guided to the integration sphere is focused on the NFAD detector with the photon trigger connected to the FPGA for single photon correlation. Fig. 14 (b) shows the single photon cross-correlation result between the transmitted PRBS and received photon clicks where the peak indicate the received energy (in terms of the number of photons collected) and delay represent the time delay of the optical signal plus code delay applied to the modulation. Fig. 14 (c) shows the "Received energy change with respect to wavelength change applied to the DFB laser, with and without CO_2 injected into the integrating sphere. A clear dip in the graph corresponds to the absorption line of the CO_2 when the gas is injected into the integration sphere, without injecting CO_2 the dip does not appear. This test proves the principle of operation the receiver system.

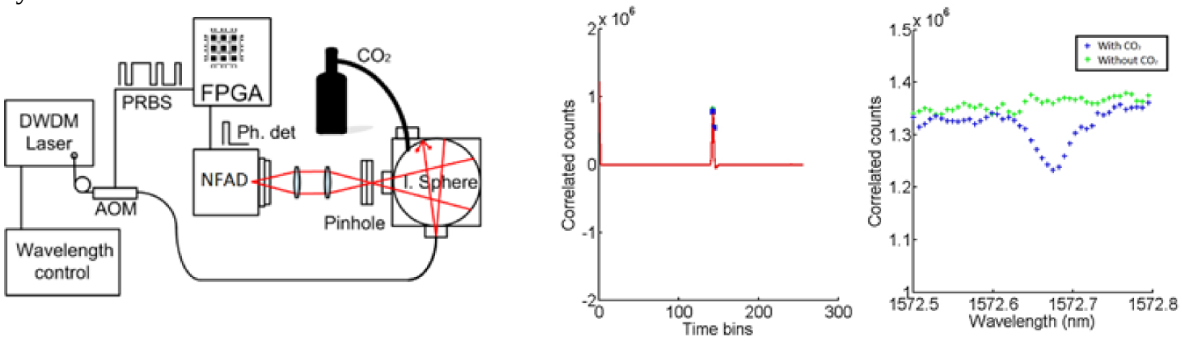

(a) (b) (c)

Fig. 14: (a) Scheme of the experiment used for CO_2 detection test. (b) Single photon cross-correlation result. (c) Cross-correlation results for different wavelengths with and without injecting CO_2 in the integrating sphere.

5. Test Campaigns

Several test campaigns have been performed along the project's execution. The purpose of these test campaigns were to validate the FSU and to perform CO_2 measurements using the BRITESPACE RM-CW IPDA lidar system in comparison with CHARM-F pulsed system [11]. Fig 15 shows some photographs taken during the test campaign of November 2014 at DLR facilities in Wessling, Germany.

(a) (b)

Fig. 15: Test campaign November 2014. (a) System receiver test setup. (b) M. Quatrevalet (DLR), P. Adamiec (ATN) and X. Ai (UBRIS) testing the FSU.

Fig. 16 shows some photographs taken during the test campaign of February 2016 at DLR's premises again. The main results obtained in these campaigns are discussed in the next subsections.

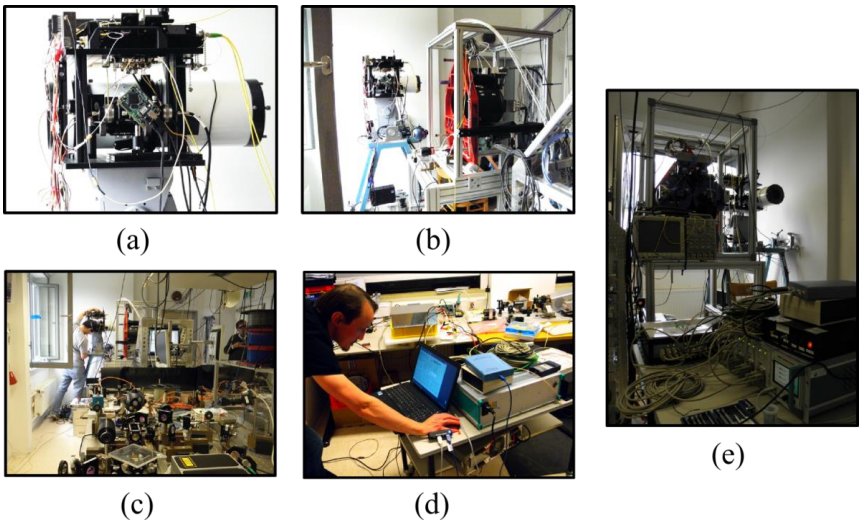

Fig. 16: Test campaign February 2016. (a) RM-CW lidar system using commercial lasers. (b) BRITESPACE system and DLR's CHARM-F system collocated measurements. (c) OPO used by the CHARM-F system. X. Ai (UBRIS) and I. Esquivias (UPM). (d) Stabilization of the BRITESPACE module experiment. P. Adamiec (ATN) (e) FSU operating with the RM-CW lidar system.

5.1. Validation of the FSU

The FSU unit has been tested at premises of DLR. It was tested in two campaigns: the initial one, which reveals some weak points of the design, and the final, where the weak points were eliminated. There are three lasers to be stabilized:

- Master laser – locked to the CO_2
- ON-line laser – shifted 350 MHz ± 350 MHz from the CO_2 line
- OFF-line laser – shifter about 10 GHz from the CO_2 line.

The most important is the stability of the master laser, because this is the limit for the ON- and OFF-line lasers. Therefore master laser (ML) was locked to the CO_2 cell and the beat between the ML and referenced laser (locked to frequency comb) was registered during several hours. The schematics of the experimental setup are shown in Fig. 17. Allan deviation of the overnight measurements is shown in Fig. 18 (a), whereas the raw date at the Fig. 18 (b). The stabilization is of about 18 kHz at the interval of 23 s and stays around 20 kHz up to 50 s. This is the direct confirmation that the improvements we have applied to the system were correct ones. Besides, it determines the lower limit of the stabilization for the ON-line laser with this system, which is 18 kHz. We can also see that the RMS is less than 0.3 MHz and reproducibility less than 1 pm and the PSD analysis shows that the ML exhibits white noise. These measurements were done in the lab with frequency comb (Menlo systems FC1500 Optical Frequency Synthesizer).

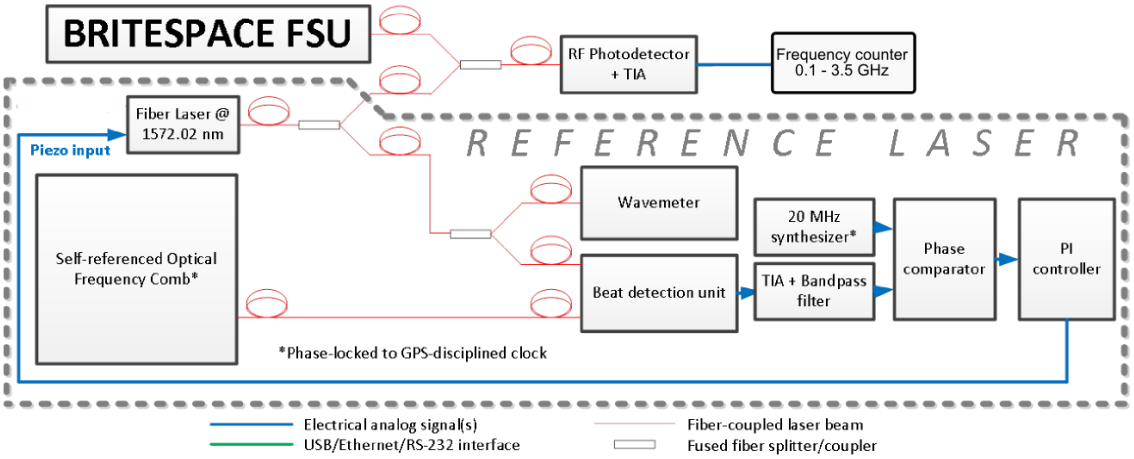

Fig. 17: Experimental setup for testing the frequency stability provided by the FSU.

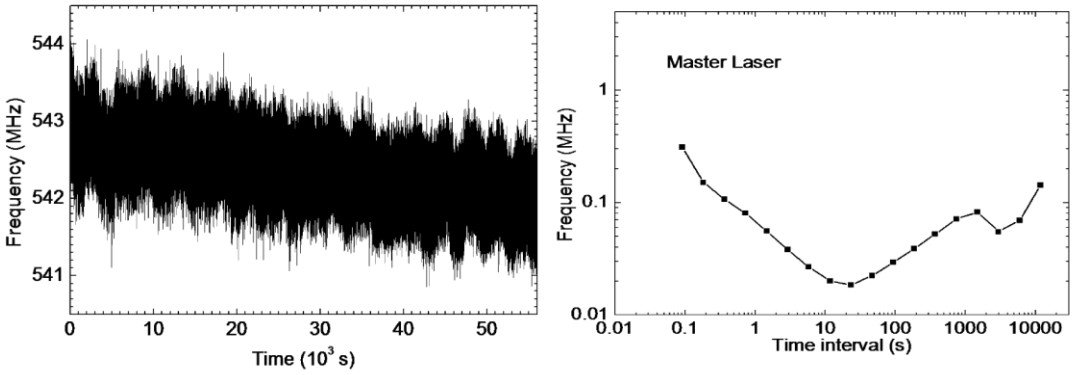

(a) (b)

Fig. 18: Beat between the master laser and reference (frequency comb) in 11 Hz (left) and its Allan deviation (right).

We have obtained the locking with both types of lasers: built-in DFB and MOPAs. It has been shown that the master laser has the stability of 18 kHz in more than 20 s, which means the demands of the project for the limits of stabilization has been fulfilled. The results for ON-line laser and also for MOPA ON-line DFB are above the specifications, but this is mainly to the fact that there was no possibility to optimize these loops for best performance. However, the measurements confirm that both lasers can be stabilized down to 18 kHz, which is the limit of the FSU. The OFF-line laser after lock provides very good stability of 53 kHz which is much better then requested 2 MHz for OFF-line stability. Both ON-line and OFF-line lasers are working with the same locking principles; therefore the results should be very similar, although we have not obtained it. This is additional confirmation that the further optimizations will allows reaching the stabilization demanded by the project. In case of the MOPA, there is additional factor as the output power from the DFB side. We expect that if the MOPAs deliver more optical power at DFB side we will be able to lock the MOPAs with much better stability, probably in the same range as master laser after optimization.

5.2. Co-located CO_2 measurements with CHARM-F pulsed system

The output power provided by the MOPAs was less than scheduled and it was decided to test the proof of concept using as transmitters two commercial DFB externally modulated with Acousto-optic modulators (AOM) and amplified by a commercial L-band EDFA. The schematic of the complete system is shown in Fig. 19. The average output power for each sounding frequency after the amplification is around 0.5 W. During February 2016, a test campaign was performed at DLR premises. The BRITESPACE system, using commercial lasers, was tested in comparison with

CHARM-F system [http://www.dlr.de/pa/en/desktopdefault.aspx/tabid-8858/15305_read-42431/]. Both systems were operating at the same time as can be seen in Fig. 20 (a). The trail path was 2 km. Fig. 20 (b) shows the retrieved dry-air CO_2 volume mixing ratio along the DLR trial path using the BRITESPACE RM-CW system (black, solid) and using CHARM-F's two receivers (blue, APD, light blue, PIN diode), compared to the expected value calculated from the in-situ measurements (black, dotted). A time-varying offsets of up to +/-10% were observed on the BRITESPACE system results, attributed to speckle effects due to the fixed target, which should be not present in airborne measurements. These results demonstrate for the first time the validity of an IPDA lidar system based on the CW Random Modulation of semiconductor lasers, together with Single Photon Counter at the receiver.

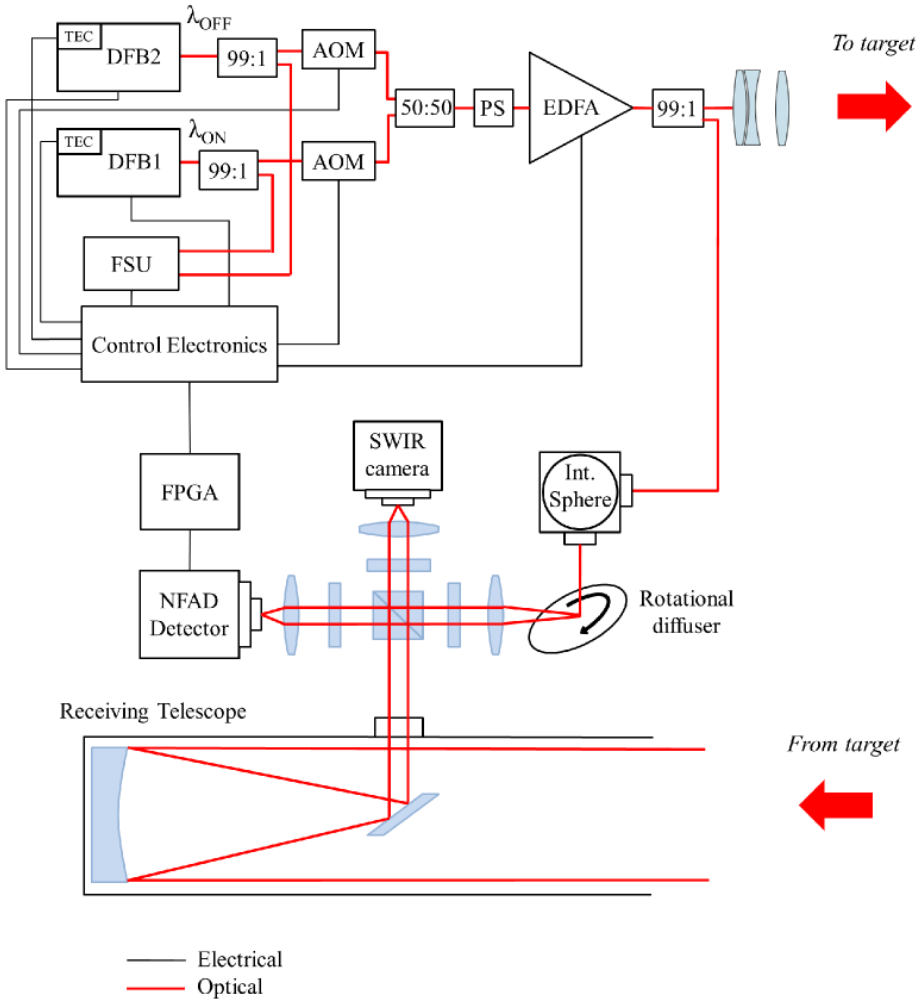

Fig. 19: Schematic of the complete system using commercial lasers and an EDFA. This system was used to perform CO2 measurements together with DLR's pulsed system CHARM-F.

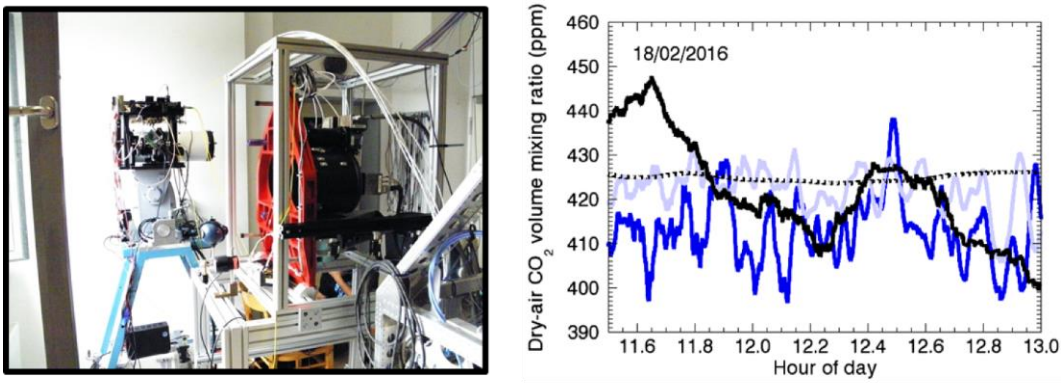

(a) (b)

Fig. 20: (a) Co-located measurements of the BRITESPACE RM-CW lidar system and DLR's CHARM-F pulsed system. (b) Retrieved dry-air CO_2 volume mixing using the BRITESPACE RM-CW system (black, solid) and using CHARM-F's two receivers (blue, APD, light blue, PIN diode), compared to the expected value calculated from the in-situ measurements (black, dotted).

6. Conclusions

Summary of final results and their potential impacts and use

The main results are directly related to the initial goals and can be summarized as follows:

- A complete system for CO_2 DIAL measurements using semiconductor lasers under Continuous Wave Random Modulation, and Single Photon Detection has been designed, implemented and tested in comparison with standard pulsed system. The results of the on-ground test at a range of 2 km showed the validity of the approach.
- The system have been analyzed and simulated; as a consequence of the experimental results and theoretical analysis, the architecture and specifications of future transmitters and RM-CW systems have been determined. The main limitation of RM-CW systems in comparison with pulsed system was found the background and detector noise, but they can be compensated using narrow filtering together with Single Photon Detection.
- The laser transmitter module based on a three section MOPA has been designed, fabricated and tested. The bent geometry to avoid coupled cavity effects resulted in single mode and stable emission spectra. The results showed the validity of the approach regarding the performance in terms of simultaneously achieving output power, beam quality, modulation capability and spectral properties.
- The fabricated MOPAs are promising devices for space-born application, as they were not degraded after a radiation dose equivalent to 50 krad.
- A Frequency Stabilization Unit based on three DFB lasers and the corresponding feedback loops (master laser locked to CO_2 line; on-line channel; off-line channel) has been designed, implemented and tested, demonstrating the frequency stability required by the application.
- In the fabricated devices, the maximum output was limited by thermal effects, and suggestions of new designs to reduce the internal heating have been proposed and simulated.
- A Quasi-3D CW simulation model for tapered semiconductor amplifiers has been developed and a 1-D Travelling Wave dynamic model has been adapted for multi-section lasers. Both have being used for better physical understanding of the MOPAs and for the proposal of new designs.

In summary, we have demonstrated the application of semiconductor lasers as convenient optical sources in such an important space application as remote sensing of atmospheric CO_2, which simultaneously requires high power and beam quality, and excellent spectral properties. Other relevant results are the demonstration of different key technologies for active sensing (detectors, system, transmitters). These results have potential impacts at different levels:

- At technological level, this would pave the way for the direct use of semiconductor lasers in other space applications, improving the capacity of European companies and research centres to lead future innovations in this field.
- At scientific level, the high degree of innovation of the project would provide new advances in the design and applications of Photonic devices and systems.
- At social level, the advances in technologies enabling a faster, cheaper and more reliable monitoring of the greenhouse gases distribution in the atmosphere should help in the struggle against global warming.

REFERENCES

[1] E. Browell, S. Ismail, and W. Grant, "Differential absorption lidar (DIAL) measurements from air and space," *Applied Physics B* **67**(4), pp. 399-410 (1998).

[2] A. Fix, G. Ehret, J. Löhring, D. Hoffmann, and M. Alpers, "Water vapor differential absorption lidar measurements using a diode-pumped all-solid-state laser at 935 nm," *Applied Physics B* **102**(4), pp. 905-915 (2011).

[3] K. Numata, J.R. Chen, S.T. Wu, J.B. Abshire, and M.A. Krainak , "Frequency stabilization of distributed-feedback laser diodes at 1572 nm for lidar measurements of atmospheric carbon dioxide," *Applied Optics* **50**(7), pp.1047-1056 (2011).

[4] B. Sumpf, K.-H. Hasler, P. Adamiec, F. Bugge, F. Dittmar, J. Fricke, H. Wenzel, M. Zorn, G. Erbert, and G. Trankle, "High-brightness quantum well tapered lasers," *IEEE Journal of Selected Topics in Quantum Electronics* **15**, pp. 1009-1020 (2009).

[5] C. Fiebig, G. Blume, M. Uebernickel, D. Feise, C. Kaspari, K. Paschke, J. Fricke, H. Wenzel, and G. Erbert, "High-power DBR-tapered laser at 980 nm for single-path second harmonic generation," *IEEE Journal of Selected Topics in Quantum Electronics* **15**, pp.978-983, (2009).

[6] H. Wenzel, S. Schwertfeger, A. Klehr, D. Jedrzejczyk, T. Hoffmann, and G. Erbert, "High peak power optical pulses generated with a monolithic master-oscillator power amplifier," *Optics Letters* **37**, pp. 1826-1828 (2012).

[7] G. Ehret, C. Kiemle, M. Wirth, A. Amediek, A. Fix, and S. Houweling, "Space-borne remote sensing of CO_2, CH_4, and N_2O by integrated path differential absorption lidar: a sensitivity analysis," *Applied Physics B* **90**(3), pp. 593-608 (2008).

[8] N. Takeuchi, N. Sugimoto, H. Baba and K. Sakurai, "Random modulation cw lidar", *Applied Optics* **22**(9), 1382-1386 (1983).

[9] X. Ai, R. Nock, J.G. Rarity, and N. Dahnoun, "High-resolution random-modulation CW lidar," *Applied Optics* **50**, pp. 4478-4488 (2011).

[10] M. Faugeron, M. Vilera, M. Krakowski, Y. Robert, E. Vinet, P. Primiani, J.-P. Le Goec, O. Parillaud, A.Pérez-Serrano, J.M.G. Tijero, G. Kochem, M. Traub, I. Esquivias, and F. van Dijk, "High power three-section integrated master oscillator power amplifier at 1.5 µm," *IEEE Photonics Technology Letters* **27**, pp. 1449-1452 (2015).

[11] A. Amediek, A. Fix, M. Wirth and G. Ehret, "Development of an OPO system at 1.57 µmfor integrated path DIAL measurement of atmospheric carbon dioxide," *Applied Physics B* **92**, pp.295-302 (2008).

[12] J.F. Campbell, N.S. Prasad, and M.A. Flood. "Pseudorandom noise code–based technique for thin-cloud discrimination with CO2 and O2 absorption measurements." *Optical Engineering 50*(12), 126002 (2011).

[13] L.S. Rothman *et al*, "The HITRAN2012 molecular spectroscopic database," *Journal of Quantitative Spectroscopy & Radiative Transfer* **130**, pp. 4-50 (2013).

[14] X. Ai, M. Quatrevalet, A. Pérez-Serrano, R.W. Nock, N. Dahnoun, I. Esquivias, G. Ehret and J.G. Rarity, "Analysis of a pseudo-random single photon counting differential absorption lidar system for space-borne atmospheric CO_2 sensing," *in preparation* (2016).

[15] J. Caron and Y. Durand, "Operating wavelengths optimization for a spaceborne lidar measuring atmospheric CO_2," *Applied Optics* **48**, pp. 5413-5422 (2009).

[16] M. Spreemann, M. Lichtner, M. Radziunas, U. Bandelow, and H. Wenzel, "Measurement and simulation of distributed-feedback tapered master-oscillator power amplifiers," *IEEE Journal of Quantum Electronics* **45**, pp.609-616 (2009).

[17] M. Vilera, A. Pérez-Serrano, J.M.G. Tijero, and I. Esquivias, "Emission characteristics of a 1.5- µm all-semiconductor tapered master oscillator power amplifier," *IEEE Photonics Journal* **7**, 1500709, April 2015.

[18] M. Faugeron, M. Tran, O. Parillaud, M. Chtioui, Y. Robert, E. Vinet, A. Enard, J. Jacquet, and F. Van Dijk, "High-Power Tunable Dilute Mode DFB Laser With Low RIN and Narrow Linewidth", *IEEE Photonics Technology Letters* **25**(1), 7-10 (2013).

[19] L. Hou, M. Haji, J. Akbar, and J. H. Marsh, "Narrow linewidth laterally coupled 1.55 µm AlGaInAs/InP distributed feedback lasers integrated with a curved tapered semiconductor optical amplifier," *Optics Letters* **37**, pp.4525-4527 (2012).

[20] A. Pérez-Serrano, M. Vilera, J. Javaloyes, J.M.G. Tijero, I. Esquivias, and S. Balle, "Wavelength jumps and multimode instabilities in integrated master oscillator power amplifiers at 1.5 µm: Experiments and theory," *IEEE Journal of Selected Topics in Quantum Electronics* **21**, 1500909, (2015).

[21] M. Vilera, A. Pérez-Serrano, M. Faugeron, J.M.G. Tijero, G. Kochem, M. Traub, M. Krakowski, F. van Dijk, S. Balle and I. Esquivias, "Modulation characteristics of a three-section MOPA," *in preparation* (2016).

[22] J. M. G. Tijero L. Burruel M. Vilera, A. Pérez-Serrano and I. Esquivias, "Analysis of the performance of tapered semiconductor optical amplifiers: Role of the taper angle", *Optical and Quantum Electronics* **47**(6), pp. 1437-1442 (2015).

A. List of BRITESPACE publications

- J. M. G. Tijero L. Burruel M. Vilera, A. Pérez-Serrano and I. Esquivias, "Analysis of the performance of tapered semiconductor optical amplifiers: Role of the taper angle", *Optical and Quantum Electronics* **47**(6), pp. 1437-1442 (2015).
- M. Vilera, A. Pérez-Serrano, J.M.G. Tijero and I. Esquivias, "Emission Characteristics of a 1.5 μm All Semiconductor Tapered Master Oscillator Power Amplifier", *IEEE Photonics Journal* **7**(2), 1500709 (2015).
- A. Pérez-Serrano, M. Vilera, J. Javaloyes, J.M.G. Tijero, I. Esquivias and S. Balle, "Wavelength Jumps and Multimode Instabilities in Integrated Master Oscillator Power Amplifiers at 1.5 μm: Experiments and Theory", *IEEE Journal of Selected Topics in Quantum Electronics* **21**(6), 1500909 (2015).
- M. Faugeron, M. Vilera, M. Krakowski, Y. Robert, E. Vinet, P. Primiani, J. P. Le Goëc, O. Parillaud, A. Pérez-Serrano, J. M. G. Tijero, G. Kochem, M. Traub, I. Esquivias and F. Van Dijk, "High Power Three-Section Integrated Master Oscillator Power Amplifier at 1.5 μm", *IEEE Photonics Technology Letters* **27**(13), pp. 1449-1452 (2015).
- M. Vilera, M. Faugeron, A. Pérez-Serrano, J. M. G. Tijero, M. Krakowski, F. van Dijk and I. Esquivias, "Three-section master oscillator power amplifier at 1.57 um for LIDAR measurements of atmospheric carbon dioxide". *Proceedings of SPIE* **9767**, Novel In-Plane Semiconductor Lasers XV, 97671K (March 7, 2016); doi:10.1117/12.2212487.
- A. Pérez-Serrano, M. Vilera, I. Esquivias, M. Faugeron, M. Krakowski, F. van Dijk, G. Kochem, M. Traub, P. Adamiec, J. Barbero, X. Ai, J. Rarity, M. Quatrevalet, and G. Ehret. "Atmospheric CO2 Remote Sensing System based on High Brightness Semiconductor Lasers and Single Photon Counting Detection". *Proceedings of SPIE* **9645**, Lidar Technologies, Techniques, and Measurements for Atmospheric Remote Sensing XI, 964503 (October 20, 2015); doi:10.1117/12.2194345.
- I. Esquivias, A.Consoli, M. Krakowski, M. Faugeron, G. Kochem, M. Traub, J. Barbero, P. Fiadino, X. Ai, J. Rarity, M. Quatrevalet and G. Erhet. "High-brightness all semiconductor laser at 1.57 μm for space-borne lidar measurements of atmospheric carbon dioxide: device design and analysis of requirements". *Proceedings of SPIE* **9135**, Laser Sources and Applications II, 913516 (May 1, 2014); doi:10.1117/12.2052191
- J.M.G. Tijero, L. Borruel, M. Vilera, A. Consoli, and I. Esquivias, "Simulation and geometrical design of multi-section tapered semiconductor optical amplifiers at 1.57 μm". *Proceedings of SPIE* **9134**, Semiconductor Lasers and Laser Dynamics VI, 91342A (May 2, 2014); doi:10.1117/12.2052488
- M. Vilera, J. M. G. Tijero, A. Consoli, S. Aguilera, P. Adamiec and I. Esquivias, "Emission regimes in a distributed feedback tapered master-oscillator power-amplifier at 1.5 μm". *Proceedings of SPIE* **9134**, Semiconductor Lasers and Laser Dynamics VI, 91340N (May 2, 2014); doi:10.1117/12.2052350
- X. Ai, R. W. Nock, N. Dahnoun, J. Rarity, A. Consoli, I. Esquivias M. Quatrevalet and G. Erhet, "Pseudo-random Single Photon Counting for Space-borne Atmospheric Sensing Applications". IEEE Aerospace Conference, Big Sky, MT, 2014, pp. 1-10 (2014). doi: 10.1109/AERO.2014.6836513

In preparation:

- X. Ai, M. Quatrevalet, A. Pérez-Serrano, R.W. Nock, N. Dahnoun, I. Esquivias, G. Ehret and J.G. Rarity, "Analysis of a pseudo-random single photon counting differential absorption lidar system for space-borne atmospheric CO2 sensing". To be submitted to Optics Express.
- M. Vilera et al. "Modulation characteristics of a three-section MOPA". To be submitted to Journal of Lightwave Technology.
- M. Quatrevalet et al. "Atmospheric CO2 Sensing with a Pseudo-random Modulation Differential Absorption Lidar System based on Semiconductor Lasers and Single Photon Counting Detection". To be submitted to IEEE Journal of Selected Topics in Quantum Electronics, special issue on Photonics for Sensing

B. List of BRITESPACE contributions to conferences

- SPIE Photonics West 2016, 13-18 February 2016, San Francisco, California, USA.
  - M. Vilera, M. Faugeron, A. Pérez-Serrano, J. M. G. Tijero, M. Krakowski, F. van Dijk and I. Esquivias, "Three-section master oscillator power amplifier at 1.57 um for LIDAR measurements of atmospheric carbon dioxide".

- BRITESPACE workshop on "Laser Diodes for Space Applications", 23-24 November 2015, Palaiseau, France.
  - I. Esquivias, M. Vilera, A. Pérez-Serrano, J. M. G. Tijero, M. Faugeron, F. van Dijk, M. Krakowski, G. Kochem, M. Traub, J. Barbero, P. Adamiec, X. Ai, J. Rarity, M. Quatrevalet and G. Ehret. "High-brightness multi-section semiconductor laser for space-borne lidar measurements of atmospheric carbon dioxide".
  - F. van Dijk, M. Faugeron, M. Krakowski, A. Larrue and M. Achouche. "Semiconductor laser development for space applications at III-V lab".

- IEEE Photonics Conference 2015, 4-8 October 2015, Reston, Virginia, USA.
  - M. Faugeron, M. Vilera, A. Pérez-Serrano, J.M.G. Tijero, I. Esquivias, M. Krakowski and F. van Dijk. "Monolithic Integration of a High Power Semiconductor Master Oscillator Power Amplifier".

- European Semiconductor Laser Workshop ESLW 2015, 24-25 September 2015, Madrid, Spain.
  - M. Vilera, M. Faugeron, A. Pérez-Serrano, J.M.G Tijero, M. Krakowski, F. van Dijk and I. Esquivias, "Performance of a Three-Section Master Oscillator Power Amplifier at 1.5 μm".
  - A. Pérez-Serrano, M. Vilera, J. Javaloyes, J.M.G. Tijero, I. Esquivias and S. Balle, "Longitudinal Multimode Instabilities in Master Oscillator Power Amplifiers at 1.5 μm".

- SPIE Remote Sensing 2015, 21-24 September 2015, Toulouse, France.
  - A. Pérez-Serrano, M. Vilera, I. Esquivias, M. Faugeron, M. Krakowski, F. van Dijk, G. Kochem, M. Traub, P. Adamiec, J. Barbero, X. Ai, J. Rarity, M. Quatrevalet, and G. Ehret. "Atmospheric CO2 Remote Sensing System based on High Brightness Semiconductor Lasers and Single Photon Counting Detection".

- 9a Reunión Española de Optoelectrónica OPTOEL '15, 13-15 July 2015, Salamanca, Spain.
  - M. Vilera, J. M. G. Tijero, P. Adamiec, A. Pérez-Serrano, M. Faugeron, M. Krakowski, F. van Dijk and I. Esquivias, "Modulation Characteristics of a Three-Section Master Oscillator Power Amplifier at 1.5 μm".
  - A. Pérez-Serrano, M. Vilera, J. Javaloyes, J.M.G. Tijero, I. Esquivias and S. Balle, "Longitudinal Multimode Dynamics in Monolithically Integrated Master Oscillator Power Amplifiers".
  - E. González, S. Aguilera, A. Pérez-Serrano, M. Vilera, J.M.G. Tijero and I. Esquivias, "Theoretical Analysis of Random-Modulation Continuous Wave LIDAR".
  - I. Esquivias, A. Pérez-Serrano, J. M. G. Tijero, M. Faugeron, M. Krakowski , F. van Dijk, G. Kochem, M. Traub, P. Adamiec, J. Barbero, X. Ai, J. Rarity, M. Quatrevalet and G. Ehret, "LIDAR System based on a High Brightness Semiconductor Laser and Single Photon Counting Detection for Space-borne Atmospheric CO2 Monitoring"

- CLEO/Europe – EQEC 2015, 21-25 June 2015, Munich, Germany.
  - M. Vilera, A. Pérez-Serrano, J. Javaloyes, J.M.G. Tijero, I. Esquivias and S. Balle, "Longitudinal Multimode Dynamics in Monolithically Integrated Master Oscillator Power Amplifiers".
  - M. Faugeron, M. Krakowski, Y. Robert, E. Vinet, P. Primiani, J.-P. Le Goëc, O. Parillaud, M. Vilera, A. Pérez-Serrano, J. M. G. Tijero, I. Esquivias and F. van Dijk, "All-Semiconductor Master Oscillator Power Amplifier at 1.5 μm for High Power Applications".
  - X. Ai, R. Nock, N. Dahnoun and J. Rarity, "FPGA High Rate Pseudo-random Single Photon Counting Correlator".

- BRITESPACE Workshop: Laser sources for LIDAR Applications, 25-26 November 2014, Wessling, Germany.
  - I. Esquivias, A. Pérez-Serrano, J.M.G. Tijero, M. Faugeron, F. van Dijk, M. Krakowski, G. Kochem, M. Traub, J. Barbero, P. Adamiec, X. Ai, J. Rarity, M. Quatrevalet, and G. Ehret, "BRITESPACE: High Brightness Semiconductor Laser Sources for Space Applications in Earth Observation".
  - X. Ai, N. Dahnoun, J. Rarity, A. Pérez-Serrano, I. Esquivias, M. Quatrevalet, and G. Ehret. "Laser power requirements for space-borne remote sensing of CO2".

- International Conference on Space Optics (ICSO 2014), 7 - 10 October 2014, Tenerife, Spain.
  - I. Esquivias, J. M. G. Tijero, M. Faugeron, F. van Dijk, M. Krakowski, G. Kochem, M. Traub, J. Barbero, P. Adamiec, X. Ai, J. Rarity, M. Quatrevalet, G. Ehret, "Random-Modulation cw lidar system for space-borne carbon dioxide remote sensing based on a high-brightness semiconductor laser".
  - M. Faugeron, M. Krakowski, Y. Robert, E. Vinet, P. Primiani, O. Parrillaud, F. van Dijk, M. F. Vilera Suarez, A. Consoli, J. M. G. Tijero, I. Esquivias, "Monolithic Master Oscillator Power Amplifier at 1.58 μm for lidar measurements".

- First International Workshop on Space-based Lidar Remote Sensing Techniques and Emerging Technologies, 08-12 September 2014, Paris, France.
  - I. Esquivias, G. Ehret, M. Quatrevalet, A. Pérez-Serrano, J.M.G. Tijero, M. Faugeron, F. van Dijk, M. Krakowski, G. Kochem, M. Traub, J. Barbero, P. Adamiec, X. Ai, and J. Rarity, "High Brightness Semiconductor Lasers as Transmitters for Space Lidar Systems".

- 24th IEEE International Semiconductor Laser Conference, 7-10 September 2014, Mallorca, Spain.
  - M. Vilera, J. M.G. Tijero, S. Aguilera, P. Adamiec, A. Consoli, and I. Esquivias, "Characterization of emission regimes in a 1.5 μm high brightness MOPA".

- 14th International Conference on Numerical Simulation of Optoelectronic Devices (NUSOD 14), 1-4 September 2014, Mallorca, Spain.
  - J. M. G. Tijero, L. Borruel, M. Vilera, and I. Esquivias, "Analysis of the performance of tapered semiconductor optical amplifiers: role of the taper angle".

- Second International Conference on Applications of Optics and Photonics (AOP14), 26-30 May 2014, Aveiro. Portugal.
  - J.M.G. Tijero, I. Esquivias, A. Consoli, M. Quatrevalet, G. Ehret, X. Ai, J. Rarity, M. Krakowski, M. Faugeron, G. Kochem, M. Traub, J. Barbero, D. López, "Remote sensing of atmospheric carbon dioxide with a random modulated CW lidar based on monolithic master-oscillator power amplifier".
  - M. Vilera, J. García Tijero, A. Consoli, S. Aguilera, I. Esquivias, P. Adamiec, "Characterization of selfpulsations in a monolithic master oscillator power amplifier".

- SPIE Photonics Europe 2014, 14 - 17 April 2014, Brussels, Belgium.
  - I. Esquivias, A.Consoli, M. Krakowski, M. Faugeron, G. Kochem, M. Traub, J. Barbero, P. Fiadino, X. Ai, J. Rarity, M. Quatrevalet and G. Erhet. "High-brightness all semiconductor laser at 1.57 μm for space-borne lidar measurements of atmospheric carbon dioxide: device design and analysis of requirements".
  - J.M.G. Tijero, L. Borruel, M. Vilera, A. Consoli, and I. Esquivias, "Simulation and geometrical design of multi-section tapered semiconductor optical amplifiers at 1.57 μm".
  - M. Vilera, J. M. G. Tijero, A. Consoli, S. Aguilera, P. Adamiec and I. Esquivias, "Emission regimes in a distributed feedback tapered master-oscillator power-amplifier at 1.5 μm".

- IEEE Aerospace Conference 2014, 1 – 8 March 2014, Big Sky, Montana, USA.
  - X. Ai, R. W. Nock, N. Dahnoun, J. Rarity, A. Consoli, I. Esquivias M. Quatrevalet and G. Erhet, "Pseudo-random Single Photon Counting for Space-borne Atmospheric Sensing Applications".

C. BRITESPACE Workshops

C.1. Workshop on "Laser Sources for Lidar Applications"

The first BRITESPACE workshop was held in Deutsches Zentrum für Luft- und Raumfahrt (DLR) Oberpfaffenhofen, Institut für Physik der Atmosphäre, Weßling, Germany, 25-26 November 2014. It was devoted to promote the contact between developers and manufacturers of laser sources with developers and users of LIDAR sytems. The number of participants on site was 40, coming from 10 different EU countries. 16 participants came from industry. The number of institutions/companies with representation at the workshop was 29, and the number of talks given was 18, with 11 invited. It was also available the remote assistance and participation. The number of remote assistants was 32, with participants from 8 countries worldwide. More details at www.britespace.eu/workshop-2014/

Fig. 18: Workshop on "Laser Sources for Lidar Applications". 25-26 November 2014. Weßling, Germany.

C.2. Workshop on "Laser Diodes for Space Applications"

The second BRITESPACE workshop was held in III-V Lab, Thales Research and Technology, Palaiseau, France, 23-24 November 2015. It was organized in collaboration with the European Space Agency (ESA). The aim was to promote the interaction between communities of laser diodes manufacturers and space systems developers and users in both research and industry environments. The number of participants was 40, coming from 7 different EU countries and Russia. 15 participants came from industry. The number of institutions/companies with representation at the workshop was 24, and the number of talks given was 19, with 12 invited. More details at www.britespace.eu/workshop-2015/

Fig. 19: Workshop on "Laser Diodes for Space Applications". 23-24 November 2015. Palaiseau, France.

D. List of acronyms

AOM – Acousto-Optic Modulator
BPM – Beam Propagation Method
CAD – Computer-Aided Design
DAOD – Differential Absorption Optical Depth
DFB – Distributed Feedback
DBR – Distributed Bragg Reflector
DWDM – Dense Wavelength Division Multiplexing
EDFA – Erbium Doped Fiber Amplifier
FSU – Frequency Stabilization Unit
FPGA – Field-Programmable Gate Array
IPDA – Integrated Path Differential Absorption
MOPA – Master Oscillator Power Amplifier
NFAD – Negative Feedback Avalanche Diode
OD – Optical Depth
PLL – Phase Locked Loop
PRBS – Pseudo Random Bit Sequence
RM-CW – Random Modulation Continuous Wave
RW – Ridge Waveguide
SMF – Single Mode Fiber
SNR – Signal to Noise Ratio
SOA – Semiconductor Optical Amplifier
SWIR – Short-Wave Infrared
TEC – Thermoelectric Cooler
TWM – Travelling Wave Model

E. Technical personnel involved in BRITESPACE

Mariafernanda Vilera, UPM
Antonio Pérez-Serrano, UPM
Antonio Consoli, UPM
José Manuel García Tijero, UPM
Ignacio Esquivias, UPM

Mickaël Faugeron, III-V
Michel Krakowski, III-V
Frédéric van Dijk, III-V

Xiao Ai, UBRIS
Richard Nock, UBRIS
Naim Dahnoun, UBRIS
John G. Rarity, UBRIS

Sarah Klein, ILT
Gerd Kochem, ILT
Martin Traub, ILT

Paola Fiadino, ATN
Pawel Adamiec, ATN
Juan Barbero, ATN
Demetrio López, ATN

Mathieu Quatrevalet, DLR
Gerhard Ehret, DLR

BRITESPACE

High Brightness Semiconductor Laser Sources for Space Applications in Earth Observation

FINAL PUBLISHABLE REPORT

APRIL 2016

The BRITESPACE consortium: